



Calcium polysulfide treatment of Cr(VI)-contaminated soil

Maria Chrysochoou*, Daniel R. Ferreira, Chad P. Johnston

Department of Civil and Environmental Engineering, University of Connecticut, 261 Glenbrook Road, Storrs, CT 06269, United States

ARTICLE INFO

Article history:

Received 1 December 2009

Received in revised form 11 March 2010

Accepted 11 March 2010

Available online 19 March 2010

Keywords:

Chromium

Reduction

Calcium polysulfide

X-ray absorption spectroscopy

ABSTRACT

Batch treatability studies for a Cr(VI)-contaminated glacial soil from a Cr plating facility were conducted using 1X and 2X the stoichiometric ratio of calcium polysulfide (CPS). The pH of the treated soil increased from 6 to 11 upon CPS addition, but progressively returned to 8–8.5 over the course of 1 year. The 1X dosage maintained a highly reducing environment up to 21 days of monitoring with the samples exposed to atmospheric oxygen, while 2X was reducing up to 180 days of curing. The EPA regulatory method for solid Cr(VI) could not reliably predict Cr(VI) in the treated solid due to ongoing reduction during the test. SPLP results showed that the CPS created an apparent Cr(VI) mobilization during the first 60 days of treatment, with subsequent decrease in soluble Cr(VI) up to 1 year of monitoring. Synchrotron micro-X-ray analyses at 60 days curing showed that Cr(VI) was predominantly bound as highly insoluble PbCrO_4 that precipitated in the interstitial pores of the soil, with very little to no Cr(VI) associated with the abundant iron oxyhydroxides. Despite its spatial accessibility and due to its low solubility, PbCrO_4 was recalcitrant to treatment, which proceeded only very slowly as judged by the SPLP data. It is concluded that, while CPS has a long residence time in the environment and is a promising reductant, in situ reduction is not an efficient treatment method for soils with highly insoluble Cr(VI) compounds, especially in surficial layers such as the one studied.

© 2010 Elsevier B.V. All rights reserved.

1. Introduction

Chromium is one of the most frequently detected metal contaminants in federal facilities, both in Department of Energy (DoE) and Department of Defense (DoD) sites. It is also frequently found in industrial facilities, such as the metallurgic, tanning and plating industries. Much is known about the fate and transport of Cr in soil and aquatic environments. Rai et al. [1] summarize the main attributes of the environmental chemistry of Cr. Toxic and carcinogenic hexavalent chromium (Cr(VI)) is mobile at neutral and alkaline pH and forms few precipitates, thus it is mobile in most soils. In oxic acidic soils it adsorbs on iron and aluminum oxyhydroxides and its mobility is reduced. Cr(VI) reduction to non-toxic Cr(III) is facilitated by naturally occurring sulfides, ferrous iron and soil organic matter. The Cr(III) precipitates as amorphous, insoluble hydroxide at pH values greater than 5.

In Cr(VI)-contaminated sites, remedial approaches have included in situ chemical reduction, monitored natural attenuation under appropriate geochemical conditions [2,3] and bioremediation [4]. The most common approach is the use of inorganic electron donors to reduce Cr(VI) and subsequently immobilize it as insoluble chromium hydroxide. Iron-based reduc-

ing agents such as ferrous sulfate, zero-valent iron (ZVI), and pyrite have been previously used [5]. However, these methods can have adverse effects due to the imparted acidity on the soil, are most effective under acidic conditions that are not favorable for Cr(III) immobilization and are costly to apply for source treatment as they are generally solid and thus not injectable. Other common reductants are sulfides delivered as liquid or gas and organic materials, such as molasses and emulsified vegetable oil. The literature on Cr treatment technologies is too extensive to effectively summarize here; a comprehensive list of relevant documents can be found at the relevant EPA website (http://www.clu-in.org/contaminantfocus/default.focus/sec/chromium_VI/cat/Treatment.Technologies/).

This study investigates the use of calcium polysulfide (CPS) as a promising alternative that is inexpensive and can be effective under a range of pH conditions. CPS is a commercially available soil additive and has been used in field applications for contaminated soil treatment; Storch et al. [6] reported on the field application of CPS to reduce Cr(VI) at a former chrome plating facility in Arizona; FRTR [7] lists the use of CPS to treat chromium in a railroad embankment with Cr-laden pigment in Morses Pond Culvert, MA; IETEG [8] described a field application at a wood treatment facility in Ukiah, CA; Charboneau et al. [9] mentions the application of CPS at the Hanford site. Even though these applications indicated that CPS could be an effective reductant, no peer-reviewed literature was found that methodically investigated the application of

* Corresponding author. Tel.: +1 860 486 3694; fax: +1 860 486 2298.
E-mail address: maria.chrysochoou@uconn.edu (M. Chrysochoou).

CPS in soil as a function of pH, Cr speciation and other geochemical parameters in bench scale studies. The only peer-reviewed literature identified was on the use of CPS to treat chromite ore processing residue (COPR) [10–12]. X-ray absorption near edge structure (XANES) analyses in COPR studies showed that while dissolved Cr(VI) was successfully treated, solid Cr(VI) concentrations remained high [11]. Thus, a thorough investigation on the use of CPS in Cr(VI)-contaminated soils is warranted.

The site at the focus of this study is a chrome plating facility in northeastern Connecticut. The history of the site is described in detail elsewhere [3,13,14]. Briefly, drippings from the Cr plating process and wastewater that was directly discharged into the adjacent wetland caused Cr contamination of the soil and groundwater. A pump-and-treat system was installed to contain the groundwater contamination and prevent migration of Cr into the wetland and adjacent river. However, previous studies at this site indicate that 99% of the chromium is tightly bound to the soil, resulting in slow leaching rates that render the aquifer treatment inefficient over a practical timescale [14]. Thus, direct treatment of the soil phase emerged as a cost-effective alternative. The objective of this study is to evaluate the use of CPS for Cr(VI) treatment in soil by investigating the pH and Cr(VI) speciation effects on the kinetics of the CPS-soil reaction.

2. Materials and methods

2.1. Site description and sampling techniques

The facility is located on the edge of an escarpment formed by glacial deposits that slopes down to a heavily vegetated wetland formed on the flood plain of the adjacent Little River. The site is underlain by a glaciofluvial aquifer and a well-graded silty and clayey-sand soil matrix that is typical of New England morphology.

Soil sampling was conducted in February 2008 with a Geoprobe™ drill rig at four locations within the perimeter of the chromium plume. Two cores were taken adjacent to the building, where the bulk of the Cr(VI) source is. They are denoted S-1 and S-2, and reached depths of 40 ft and 20 ft, respectively, with the water table at a depth of approximately 28 ft S-2 was advanced only down to 20 ft because of a large boulder encountered at that depth. Additionally, 4–5 kg of sample was collected with a hand auger (denoted as HA) to a depth of roughly 4 ft in the unsaturated zone near the building. The cores were separated into fractions representing 4 ft increments of depth and all samples were homogenized and stored in sealed plastic bags at 4 °C. Samples are denoted by core source and depth increment in ft, e.g. S-1 (28–32).

2.2. Soil characterization

Total Cr(VI) analysis was conducted according to methods EPA 3060A and EPA 7196.

SPLP analysis was conducted according to EPA method 1312. Total Cr in the SPLP leachate was analyzed by Phoenix Environmental Labs (Manchester, CT) by EPA method 6010B. Particle size analysis was conducted according to method ASTM D422. Soil pH analysis was conducted according to method ASTM D4980-89 and water content by method ASTM 2216-98. XRF analysis of the soil was conducted according to EPA 6200. Total metal and total organic carbon analyses conducted by Phoenix Environmental Laboratories in Manchester, CT according to EPA methods 3015A, 6010B and 9060.

X-ray diffraction (XRD) analysis was performed using a Bruker D5005 diffractometer with Bragg Brentano geometry using CuK α radiation at 2 θ angles between 5° and 65°, with a step size of 0.02° and scanning time of 3 s per step. Samples were pulverized, passed

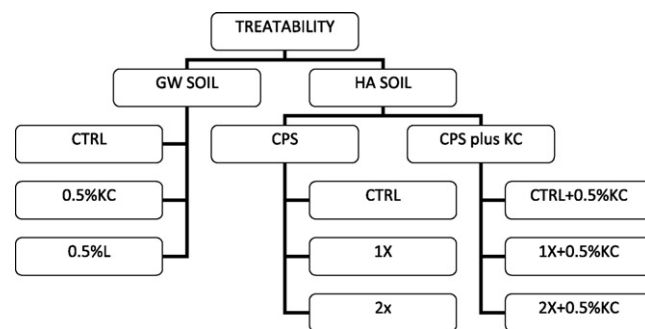


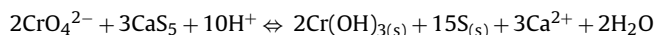
Fig. 1. Overview of treatability matrix (GW=soil under the groundwater table, HA=surficial soil collected with a hand auger, CPS=calcium polysulfide, L=lime, KC=K₂CO₃, 1X=stoichiometric dosage to reduce Cr(VI) in the soil, 2X=double the stoichiometric dosage).

through a U.S. 400 sieve (38 μ m), and contained 20 wt.% corundum as an internal standard. XRD data analysis was performed with the Jade software (Materialsdata Inc.), version 8.5, with reference to the International Center for Diffraction Data database [15].

2.3. Treatment design

The site characterization study revealed an uneven vertical distribution of chromium, with the majority of Cr(VI) contamination confined to the near-surface layer (~5 ft depth), whereas Cr(III) was the primary species at depths below 28 ft where the groundwater table was observed (see Section 3.1). Based on these results, the treatability study was split into two parts, addressing the soil underneath the groundwater table and the near-surface soil separately. The notation for the two soil zones is HA (for the surficial sample collected with the hand auger) and GW for the soil collected from the groundwater zone. The GW soil was treated with a pH buffering agent (K₂CO₃) alone, in order to investigate whether Cr(III) immobilization at alkaline pH would be sufficient to reduce Cr mobility below the CT regulatory limit of 0.11 mg/L Cr for non-drinking water aquifers. The HS soil was treated with CPS with and without a buffering agent, to investigate whether the addition of an alkaline agent would further facilitate Cr(VI) mobilization from the soil for reductive treatment. An overview of the experimental matrix is given in Fig. 1.

The theoretical oxidation–reduction reaction between Cr(VI) and CPS under anaerobic conditions is:



Based on this reaction stoichiometry, the 29% CPS solution concentration, and an average HA sample Cr(VI) concentration of 7852 mg/kg, 156 mL of CPS solution were required per kg dry soil for a 1X stoichiometric relationship and 312 mL for 2X. Batch tests were conducted by placing 300 g of dry soil sieved through a No. 4 sieve (2 mm) in sealed plastic jars and the required CPS solution and kept at a 1:1 liquid to solid (L:S) ratio. Saturated source zone samples were treated with a 0.5% K₂CO₃ (KC) solution and a 0.5% lime (L) solution for comparison. The amounts of potassium carbonate and lime were determined by conducting a preliminary pH buffering study with varying amounts of these agents. All studies were performed in duplicate.

The CPS product used in the study was Cascade®, a 29% CPS solution obtained from Best Sulfur Products, Inc. All other chemicals used are ACS certified reagents. Soil analyses were conducted at 0, 1, 7, 28, 60, 180 and 365 days of curing. Soil pH, redox potential, total Cr(VI) and SPLP analyses were conducted according to the methods previously described.

Table 1
Characterization results of the control samples in the shallow HA and the ground-water GW soil.

Parameter	CTRL – HA soil	CTRL – GW soil
pH	6.3	6.0
Cr(VI) (mg/kg)	7800	30
Cr(total) (mg/kg)	14,800	380
Fe (mg/kg)	25,900	9440
Al (mg/kg)	12,800	7280
Ca (mg/kg)	1000	800
Mn (mg/kg)	260	140
Pb (mg/kg) ^a	15,000	20
TOC (mg/kg)	12,000	260

^a Pb concentration obtained by XRF analysis.

2.4. X-ray absorption spectroscopy

Representative samples from the 60-day cured samples of the HA soil (CTRL, 1X and 2X without KC addition) were prepared as 30- μm thick diamond-polished thin sections by Spectrum Petrographics (Vancouver, WA) for microprobe analyses. Micro-XRF, μXRD and μXANES measurements were performed on Beamline 10.3.2 at the Advanced Light Source (ALS) [16]. Micro-XRF elemental maps were acquired at 13.5 keV incident energy with a beam size of $7\ \mu\text{m} \times 7\ \mu\text{m}$ and a counting time of 50 ms/pixel. Fluorescence counts were collected for Ca, Ti, Cr, Mn, Fe, Ni, Cu, Zn and Pb with a seven-element Ge solid-state detector. From elemental distribution maps, various spots of interest were selected for μXRD to identify crystalline phases and for Cr K-edge μXANES to probe Cr redox state. Cr chemical mapping was performed at incident energies of 5960, 5993 and 6250 eV to obtain the background, Cr(VI) and total Cr (Cr(total)) signals, respectively. Energy calibration was performed using a Cr foil (5989.02 eV) [17]. The background map was subtracted from the two others to obtain signals attributable to Cr only. Next, 7% of the Cr(total) signal was subtracted from that of Cr(VI) to account for the finite XANES signal that Cr(III) species typically exhibit at the Cr(VI) energy. The Cr(VI) and Cr(total) maps were then assembled into a composite map.

All μXANES spectra were collected in fluorescence mode, pre-edge background subtracted and post-edge normalized using custom LabView software. Three XANES standards of pure CaCrO_4 , PbCrO_4 and BaCrO_4 were obtained at the beamline; μXRD patterns confirmed that the pure chemical corresponded to 100% pure crystalline compound. Additional standards were provided as a courtesy of P. Nico and were also obtained previously at BL 10.3.2.

Microdiffraction patterns were recorded in transmission mode with a Bruker Smart6000 CCD camera at 17 keV for 5 min with a beam size of $16\ \mu\text{m} \times 7\ \mu\text{m}$. Two-dimensional patterns were radially integrated and calibrated using the Fit2d software [18] and an α -alumina standard. Analysis was performed with the Jade software v.8.5 and reference to the ICDD database.

3. Results and discussion

3.1. Soil characterization

The soil from both the HA and GW samples was well-graded sand with a slightly higher silt and clay content (12%) in the HA soil. The pH of the soil was acidic and generally decreased with depth, ranging from 6.5 to 7 close to the surface to 5.5 in the GW sample for the source samples close to the building and even below 5 in the aquifer near the extraction well.

Table 1 shows the chemical characterization results for the composite samples that were used in the treatability study. The GW sample was a mix from the 28–32 ft and 32–36 ft sampling depths and had a pH of 6. The Cr(VI) content of this composite sample was

30 mg/kg, while Cr(total) was 380 mg/kg. Thus, Cr(VI) was only 9% of the total chromium in the groundwater zone. This is attributed to the acidic pH conditions that historically prevailed in the soil, and which favored retardation of Cr(VI) in the upper zones and leaching of Cr(III) into the deeper soil. Nikolaidis et al. [13] reported a vertical pH profile that ranged from 3.0 at 25 ft depth up to 5.5 close to the ground surface. This extreme soil acidity was due to the acidic solutions that leached through the facility floor, as well due to the discharged wastewater, both of which were the primary sources of contamination. The soil pH apparently rebounded by almost two pH units over the course of the 15 years that elapsed between the two studies. The mechanism of pH buffering cannot be elicited from the comparison of the two studies, as soil chemistry and mineralogy appears to be the same. Potential buffering processes are deprotonation of the abundant iron hydroxide surfaces, precipitation of calcite (observed by XRD in small amounts) and microbial activity [19].

The Cr(VI) concentration was high (7800 mg/kg) in the HA sample, while individual samples were found to have up to 10,000 mg/kg Cr(VI). The total Cr was at 14,800 mg/kg in the HA sample, so that Cr(VI) was approximately 50% of the total chromium. The HA soil was also found to have considerably higher Fe and TOC content compared to the saturated zone, along with a high Pb content of 15,000 mg/kg. The presence of Pb was a surprising finding, as it was not reported in previous studies and its source was not apparent based on the Cr plating processes. The Pb concentration was only high at the top 5 ft and quickly declined to background concentration of ~ 20 mg/kg. The saturated soil appeared to be closer to clean sand with lower contents of all major metals. Mn concentrations were low in all zones, so that Mn-induced reoxidation of Cr(III) is not expected to be significant for treatment considerations.

XRD analysis showed that quartz was the predominant soil mineral, with plagioclase and potassium feldspar and some mica as secondary minerals. Traces of kaolinite clay were observed in the shallow soil, along with some crystalline ferrihydrite and calcite.

3.2. pH buffering study for saturated soil

Fig. 2 shows the pH and SPLP results for the buffered saturated soil. The control sample maintained pH 6 over the course of 1 year, while the addition of potassium carbonate led to a constant pH of ~ 10 , which is the $\text{pK}_{\text{a}2}$ value for the carbonate system [20]. Lime raised the pH to 12.4, which is the pH of lime-saturated water [21], but in this case the pH decreased to 9 between 60 and 365 days of curing.

The addition of 0.5% lime corresponds to the addition of 0.18 equiv. OH^- /kg soil, while the addition of 0.5% KC corresponds to 0.04 equiv. OH^- /kg soil, assuming that the main buffering reaction is CO_3^{2-} turning into HCO_3^- . However, lime was less successful than KC to maintain high pH in the long term.

There are two main processes that reduce pH in the amended soil over time: CO_2 sequestration and calcite formation, and release of H^+ from the protonated surfaces of iron and aluminum oxyhydroxides. Other processes such as deprotonation of organic compounds are considered to be of less importance due to their low content in the saturated soil. The desorption of protons from iron hydroxide surfaces is thought to be a fast process [19], while CO_2 sequestration is limited by the rate of diffusion of atmospheric CO_2 into the liquid phase. The buffering capacity related to proton adsorption and desorption of Fe and Al oxyhydroxides has been found to be in the range 0.04–0.4 mol/kg [22], although this referred to the pH range 3.5–8.3. Given the high Fe content of the soil in this study, pH buffering was anticipated to be substantial; however, it was not enough to counteract the effect of KC and lime addition. In the case of lime, CO_2 sequestration was accelerated by the high amounts of added calcium, which produced calcite, removing

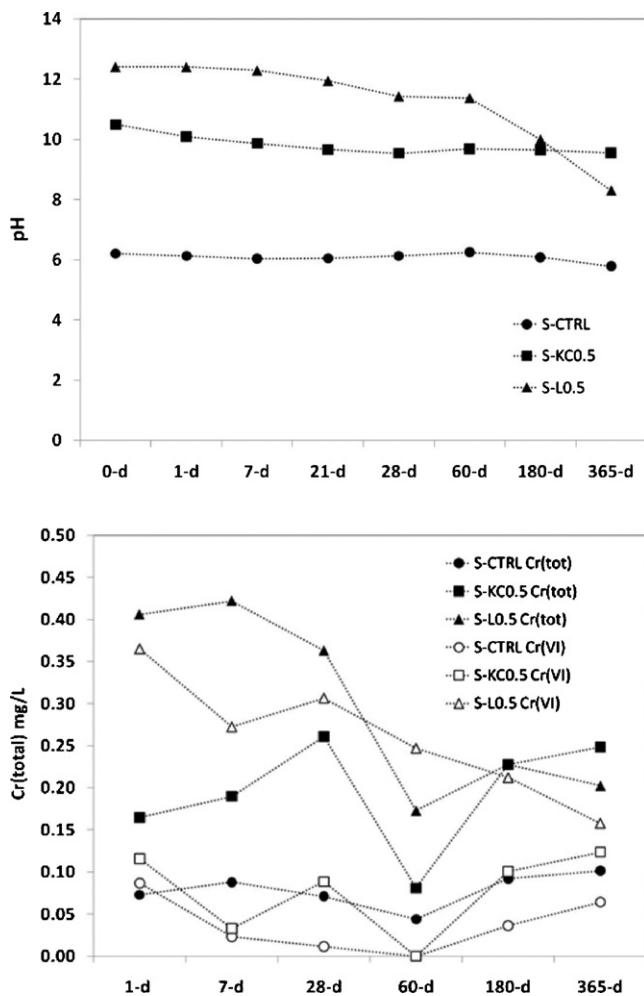


Fig. 2. pH (top) and SPLP Cr and Cr(VI) (bottom) in the buffered GW soil.

CO_3^{2-} from solution. In the KC-amended soil, CO_2 -imparted acidity would be limited by its solubility and equilibrium concentration, since Ca was too low for substantial calcite formation.

It should be noted, however, that the access to CO_2 in a field application would be more limited compared to the batch lab conditions, and thus pH decrease in the limed soil would be even slower. Furthermore, carbonate advection and retardation processes are not captured in a batch study, so that the prediction of equilibrium pH concentrations in a field aquifer would require column studies to be more precise.

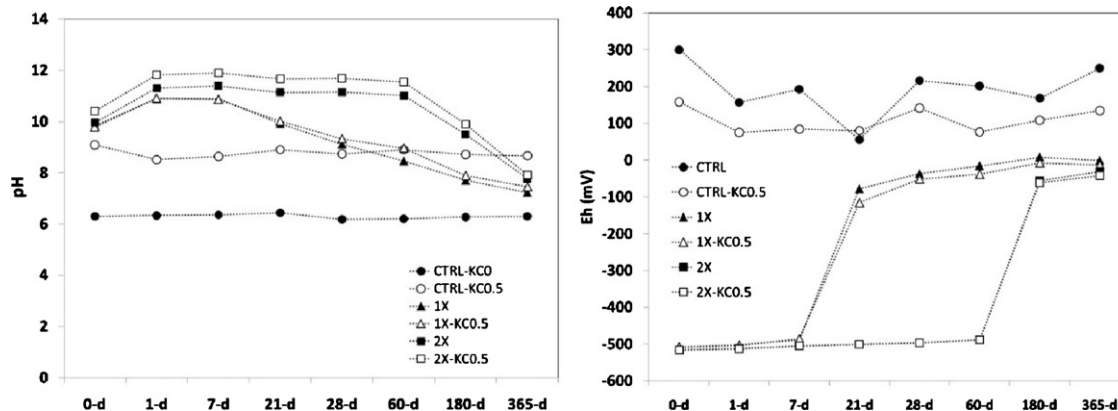


Fig. 3. pH (left) and redox potential (right) in the CPS-treated HA soil.

The addition of alkaline agents resulted in the mobilization of Cr(VI) from the saturated soil, as anticipated. However, Cr(III) immobilization under SPLP conditions was not attained. The SPLP pH of the control sample was in the range 5.5–6, while the SPLP pH of the KC and L samples was 9–9.5. Modeling of Cr(III) solubility with respect to $\text{Cr}(\text{OH})_3$ using Visual Minteq showed that the measured concentrations were almost two orders of magnitude higher than the predicted equilibrium concentration of $5 \mu\text{g/L}$. The reason for this behavior is unknown. It is possible that it is an artifact of the analytical procedures, whereby Cr(III) is calculated as the difference between Cr(total) and Cr(VI). Since the largest fraction of the mobilized Cr(total) was due to the mobilization of Cr(VI), it is possible that the error associated with the measurement of each Cr species caused an apparent increase in Cr(III) that was not real. In either case, the mobilization of Cr(VI) was such that it rendered a simple buffering treatment prohibitive. Thus, reductive treatment of the saturated zone appeared to be necessary, despite the low Cr(VI) concentrations in the solid.

3.3. CPS treatment of shallow soil

Fig. 3 shows the pH and redox potential over time in the CPS-treated unsaturated soil. The pH in the control sample remained at 6 throughout the 1-year testing period. The addition of 0.5% KC resulted in a steady increase of soil pH to approximately 9. This is a lower value compared to the saturated soil and the pK_{a2} (10.3) of carbonate. This difference is attributed to the higher iron content of the unsaturated soil and the associated buffering capacity of the iron oxyhydroxide surfaces. Consistently with the notion that proton release of these surfaces occurs fast, the pH remained at 9 immediately after the addition of KC and until the end of the testing period. The addition of CPS resulted in the increase of soil pH to ~ 11 for the 1X dosage and 11.4 for the 2X dosage (the natural pH of CPS is 11.5). All CPS-treated samples showed progressive decrease in pH down to 7.2 for 1X and 7.8 for 2X, with the addition of KC not resulting in significant change in the buffering behavior of the soil. Again, the addition of large amounts of Ca is thought to have caused increased sequestration of CO_2 to form calcite; the buffering pH of calcite is 7.3 [19] which is consistent with the observed results. In terms of in situ remediation, these results indicate that the alkalinity imparted of CPS can be buffered over time, and that the rate of buffering will be dictated by the availability of CO_2 . This process would likely take longer than 1 year in saturated conditions, where CO_2 diffusion into groundwater would be limited.

The redox potential in the control samples was oxidizing, indicating that in situ conditions at the site do not currently favor Cr(VI) reduction. The addition of CPS resulted in a sharp drop of Eh to -500 mV , at which Cr(VI) reduction to Cr(III) is favored. The Eh

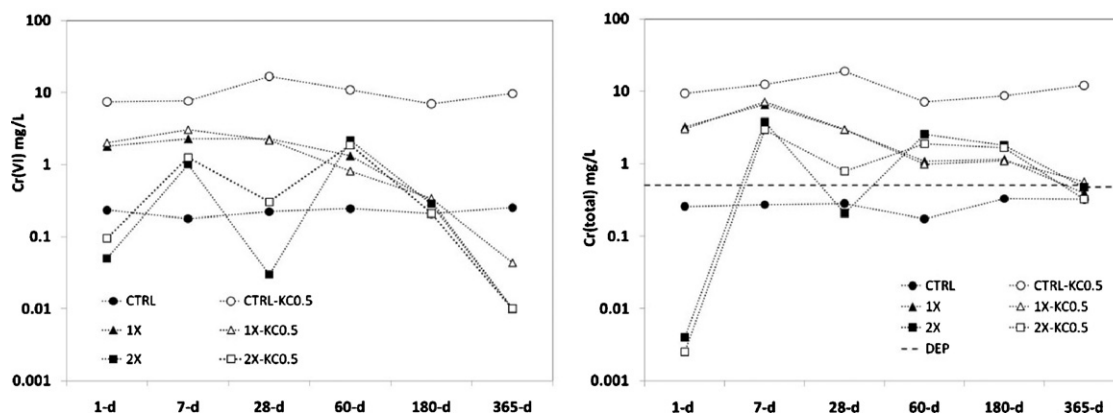


Fig. 4. SPLP Cr(VI) (left) and Cr(total) (right) concentrations in the CPS-treated HA soil.

remained highly reducing in the 1X samples until 21 days, after which it increased sharply to -70 mV and progressively to a mildly oxidizing environment. This signaled a consumption of sulfide that could be due to oxidation by chromate, by diffusing oxygen or by the natural oxidizing capacity of the solid. The 2X sample maintained a reducing environment for longer, with the Eh increasing at some point between 60 and 180 days of curing. It is recognized that subsurface conditions would not expose sulfide to as much oxygen as the batch study did and that sulfide would likely have a longer staying power. Even so, sulfide oxidation appeared to be slower compared to ferrous iron, which can be quickly oxidized in the presence of oxygen [23].

The success of the reductive treatment could not be evaluated using the EPA regulatory method for Cr(VI) measurement in the solid. While the control samples yielded constant Cr(VI) concentrations and spike recoveries over the entire curing period, CPS-treated samples consistently yielded non-detectable (<5 mg/kg) Cr(VI) concentrations, and spiked samples had recoveries of 0%. Clearly, unreacted sulfide in the samples reacted with the released Cr(VI) during the test, resulting in artificially low concentrations. Similar observations have been reported for chromite ore processing residue [24]. Thus, alkaline digestion cannot be used to assess the effectiveness of reductive treatment when the reductant has not been exhausted.

The SPLP results (Fig. 4) confirmed that the alkaline digestion results were an artifact of the test, since there was substantial leaching of Cr(VI) up to 60 days curing. Cr(VI) leaching then declined substantially in both the 1X and 2X treatments, reaching non-detectable values (<10 μ g/L) at 365 days of curing. Cr(VI) leaching was below the control sample only at the 1-year point. However, it should be stressed that the creation of alkaline conditions in the CPS samples renders them comparable to the CTRL-KC0.5 sample, in which substantial mobilization of Cr(VI) was observed due to the alkaline pH. It is therefore concluded that Cr(VI) reduction did take place, with the decreasing trend commencing after 28 days of curing in the 1X sample and after 60 days of curing in the 2X sample. These curing times coincide with the increase of the redox potential in these samples (Fig. 3), confirming that sulfide oxidation took place around that time and that chromate reduction was at least partially responsible for sulfide consumption. Thus, chromate reduction by CPS in the soil appeared to be a very slow process. Ongoing studies show that once Cr(VI) is in solution, reduction by CPS occurs very rapidly (unpublished data), so that the limiting step for Cr(VI) reduction is considered to be its release from the solid. Evidence to this end will be presented in Section 3.4.

The SPLP Cr(total) leaching levels in the CPS-treated soil also declined with time and were below the CT regulatory limit of 0.5 mg/L by 365 days of curing. However, the same surprising Cr(III)

mobilization in the CTRL-KC0.5 and the CPS-treated samples compared to the control was also observed in the HA soil, as was the case in the GW soil. The SPLP pH could again not account for this observation, as the SPLP pH of the control sample was approximately 7, while the SPLP pH of all other samples was in the range 8–9, in which Cr(III) is theoretically more insoluble. Since Cr(III) was found to be associated with amorphous and crystalline hydroxide by X-ray absorption spectroscopy, it is not apparent why the addition of KC or CPS would cause a mobilization of Cr(III) from the soil. The only plausible hypotheses at this time are (a) analytical artifacts; and (b) increased mobilization caused by physical dissolution of Cr(VI)–Cr(III) mixed grains under alkaline conditions. Overall, SPLP is not the best test to assess the mobility of metal species under in

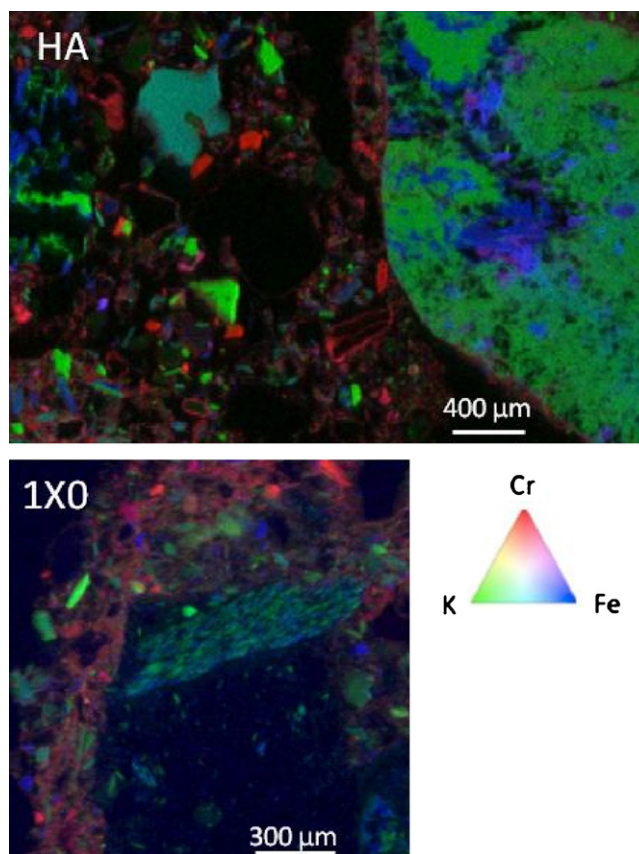


Fig. 5. Tricolor XRF maps of untreated HA sample (top) and 1X-treated HA sample at 60 days (bottom).

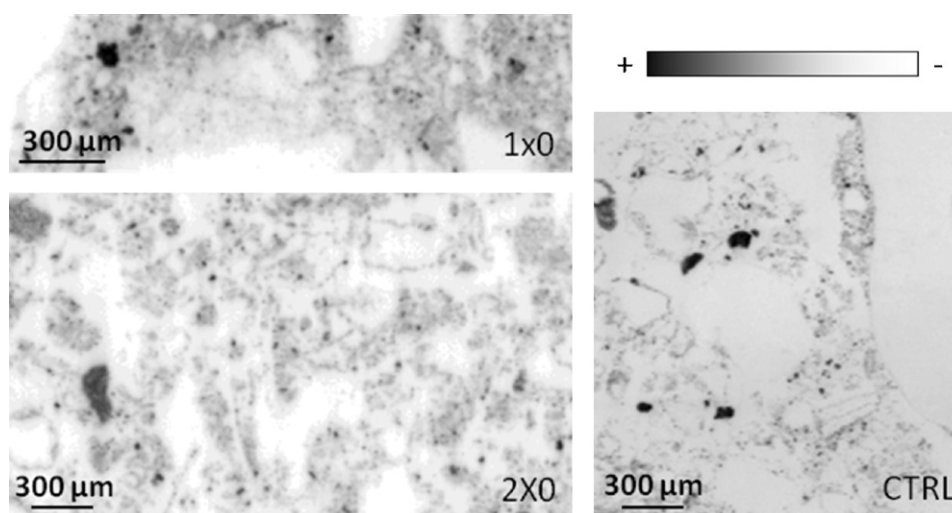


Fig. 6. Inverse grayscale Cr(VI) micro-XRF maps of the control HA sample and the samples treated with 1X and 2X CPS.

situ conditions in the soil, as both the TCLP and SPLP tests have been previously found to change metal speciation during the test in ways that were not consistent with field conditions [25,26]. However, the regulation of the site by the CT Department of Environmental Protection and the Environmental Protection Agency dictated that this test had to be conducted for regulatory purposes.

3.4. Micro-X-ray absorption spectroscopy

Micro-XRF, -XAS and -XRD analyses were conducted on samples cured for 60 days. Fig. 5 shows the distribution of Cr, Fe and K in two of three samples (untreated and 1X-treated). Fe and K were the most abundant elements and thus representative of the presence of solid grains in the sample. Cr was found to be primarily associated with finer grains, either as distinct particles, or as distinct halo on the rim of larger particles. Some Cr was found diffuse within larger grains (e.g. in the large grain of the untreated sample), but its concentration was significantly lower, so that the faint red color is difficult to see. Since thin sections yield two-dimensional images, it is difficult to say whether the diffuse Cr was located within the interior of the larger particle or if it was found adsorbed on its surface. In either case, it appears that the majority of the Cr mass was located on the rims of larger particles and in the finer grained fraction of the soil. Cr-rich particles with diameter ranging from 20 to 100 μm were observed in all three maps, with the largest ones found in the untreated sample. The Cr species associated with each type of particles was further investigated with the use of the chemical maps and XANES.

Fig. 6 shows the Cr(VI) maps for the control and the treated samples, with the intensities drawn to scale, i.e. the intensity of the color corresponds to magnitude of concentration. Table 2 shows the average pixel intensity over these three maps, as well as the corresponding Cr(total) maps of the three samples. There was variability in the average Cr(total) intensity in the three maps, which suggests that there is variability in the Cr distribution within the soil. The area captured in the control sample consisted of fewer larger grains, which tended to have less Cr, whereby the areas in the treated samples appeared to be more fine-grained and have higher Cr concentrations. One of the shortcomings of micro-X-ray analyses is that the time required to collect the μXRF maps limits the size of the areas and the number of samples that can be analyzed within the available beam time, so that sample variability becomes an issue when comparing the untreated and the treated samples. Thus, judging the success of treatment based on the average Cr(VI)

intensity was not possible, as differences were attributed to sample variability rather than redox reactions.

The ratio of Cr(VI) to Cr(total) was considered a more suitable indicator of reduction processes in the treated soil, as the total Cr presence would be normalized across different samples. Table 2 shows that the average counts of Cr(VI) were 37% of the Cr(total) in the untreated sample after 60 days of curing in aqueous solution; this value dropped to 19% in the 1X-treated and to 17% in the 2X-treated sample. Chemical analyses yielded a Cr(VI)-to-Cr(total) ratio of 50% in the control sample. The difference between this value and the 37% observed by μXRF may be either due to sample variability or due to the natural reducing capacity of the control soil; the high TOC content in the surficial soil renders organically-induced Cr(VI) reduction a viable possibility. Both treated samples appeared to have a similar level of success in reducing Cr(VI), as the difference between 17% and 19% is not considered statistically significant without looking at more samples. Even though the differences in Cr(total) concentrations make it difficult to draw definitive conclusions as to how much Cr(VI) was reduced, the reduction in the Cr(VI)/Cr(total) ratio suggested that reduction did occur and that it could be up to 50% of the original Cr(VI) content.

The distribution of counts between the pixels was very similar for the two treated samples, but had differences with the untreated sample: as an indication, 50% of the pixels accounted for 9% of the Cr counts in the treated samples and 24% of the Cr counts in the untreated sample. In other words, the distribution of pixel intensity was biased towards pixels with higher counts in the treated samples. This suggests that reduction preferentially targeted areas of low Cr(VI) concentration, while high-Cr(VI) areas remained largely intact. This suggests that high-Cr(VI) compounds were not amenable to treatment after 60 days of curing time. The comparison of the μXRF Cr(VI) maps (Fig. 6) confirms that dark spots persisted in the treated samples, whereby the 2X sample had reduced intensity and smaller dark spots. Interestingly, this is the opposite phenomenon of Cr(VI) reductive treatment of chromite ore processing residue, in which high-Cr(VI) compounds were more

Table 2

Average pixel intensity over the XRF-mapped regions for Cr(VI) and Cr(total) in the untreated vs. the treated samples of the HA soil.

	Cr(VI)	Cr(total)	Cr(VI)/Cr(total) (%)
Control – 60 days	6,700	18,000	37
1X-treated – 60 days	9,600	50,000	19
2X-treated – 60 days	4,600	27,300	17

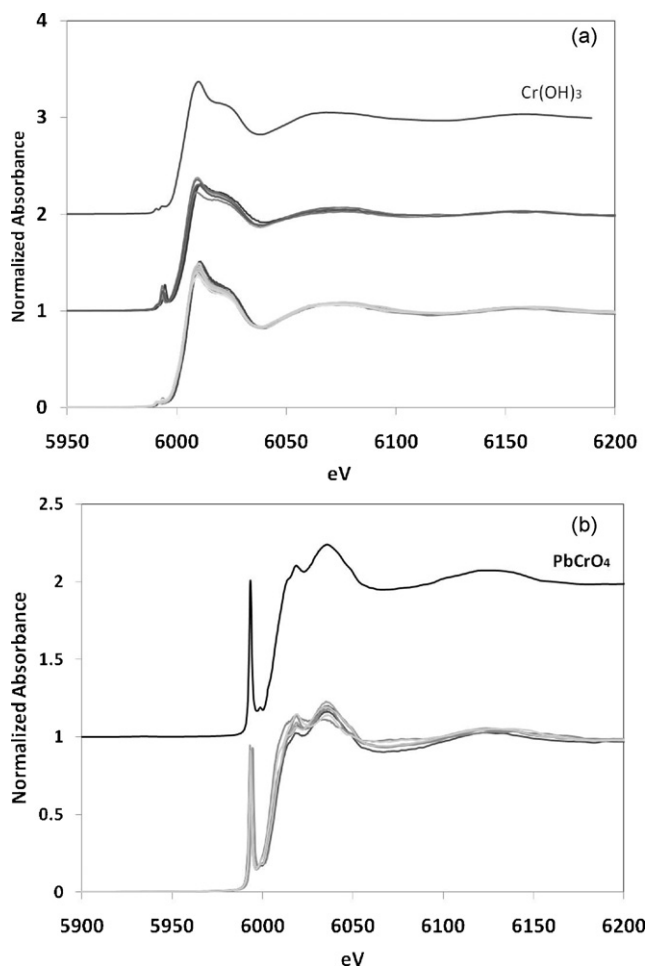


Fig. 7. XANES spectra of selected points as compared to pure Cr(OH)₃ (a) and PbCrO₄ (b) (spectra offset for clarity).

amenable to treatment [27]. Thus, different mechanisms of Cr(VI) release take place in different geochemical systems.

The speciation of Cr(VI) was also investigated by point μ XANES and μ XRD in order to further elucidate the reduction mechanisms. Twenty points were analyzed in the control sample and ten points in each of the treated samples; points were chosen to represent a variety of Cr(VI) intensities in the Cr(total) μ XRF map.

Fig. 7 shows the XANES spectra of points that resembled pure Cr(OH)₃: 8 points belonged to the control sample, 3 to the 1X-treated and 5 to the 2X-treated sample. Additionally, seven points (2 CTRL, 2 1X and 3 2X) resembled Cr(OH)₃ in the post-edge region, but still had a discernable Cr(VI) peak at 5993 eV. Based on the μ XRF maps these points were obtained from areas with high variability in the element distribution; Cr is associated with either Pb, Fe or no other element in adjacent pixels with a resolution of 10 μ m \times 10 μ m; thus, it is concluded that a physical mixture of Cr(III) and Cr(VI) compounds is responsible for the observed XANES spectra.

The majority (8 out of 13) of high-Cr(VI)-bearing points were found to very closely resemble PbCrO₄ (Fig. 7(b)). This was further confirmed by μ XRD, which showed crystalline crocoite as the only mineral found in these points. The Pb content of the soil could account for approximately half of the Cr(VI) being present as PbCrO₄ (Table 1) at the top 5 ft of the unsaturated zone, while deeper layers contained no appreciable Pb levels (<20 mg/kg). While the Pb source is not known (it is assumed that it is also the discharged wastewater and drippings), it appears that Pb migration into the deeper layers was inhibited by the formation of insoluble

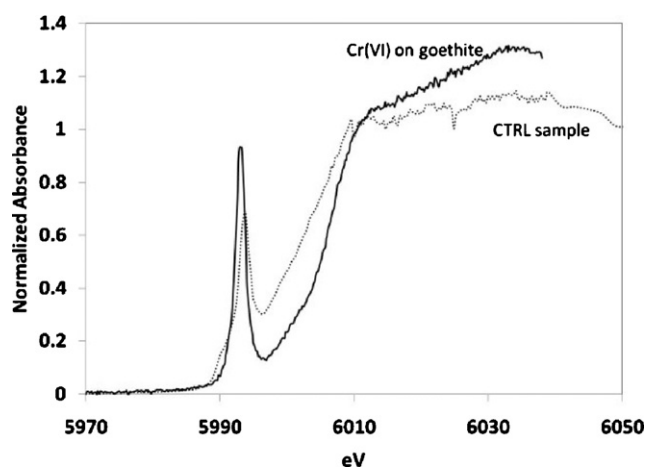


Fig. 8. XANES point of control HA sample and Cr(VI) sorbed on goethite (spectrum courtesy of Rick Wilkin, USEPA).

PbCrO₄, while Cr was present in excess and in the trivalent form, which was more mobile in the acidic soil conditions and leached to the saturated zone.

The prevalence of PbCrO₄ as the main form of Cr(VI) in the soil also explains the difficulty to treat the HA sample. Dissolution of this highly insoluble Cr(VI) compound could proceed only extremely slowly, kinetically inhibiting the reduction process. Additionally, galena (PbS) was observed in a few of the μ XRD patterns, scavenging part of the added sulfide.

The speciation of the remaining Cr(VI) points was a mixture of Cr(OH)₃ and PbCrO₄ according to linear combination fitting. This agrees with the assumption that increased Cr(III) mobilization could be attributed to the physical dissolution of mixed Cr(III)–Cr(VI) grains. Only one point could not be fitted with the available spectra and it resembled more Cr(VI) sorbed to goethite (Fig. 8). This was the only point that was taken within the interior of one large grain, while other points were located in the more fine-grained areas surrounding the large grains.

Given the bias introduced in the statistical analysis of Cr(VI) speciation by the choice of a few selected points, it was thought that the association of Cr with Fe may have been underestimated through this process, both in terms of Cr(VI) sorption as well as Cr(III) co-precipitation with Fe(III) hydroxides. The association of the two elements was further investigated by examining the correlation between the pixel values of these elements over the entire obtained maps, using the custom XRF map analysis software that was developed at BL 10.3.2. Cr(total) and Cr(VI) correlation with Fe were investigated independently. The analysis showed that Cr was not associated with Fe in the majority of the pixels. The Pearson correlation coefficient between the Fe and Cr pixel intensity was 0.33 in the 1X map, 0.32 in the 2X map and 0.11 in the control HA sample. The analysis further showed that the pixels with high correlation between the Cr and Fe values corresponded to a single isolated particle in the HA and the 1X maps, with a diameter of 50 and 80 μ m, respectively. One large (50 μ m) and several smaller (20 μ m) particles with high Fe–Cr correlation were observed in the 2X map. Thus, co-precipitation of Cr with Fe was not observed to be a dominant mechanism in this soil.

Similar observations were made for the Cr(VI)–Fe correlation. The Pearson coefficient was 0.07 in the control sample, 0.17 in 1X and 0.07 in 2X. A visual inspection of the μ XRF maps confirmed that the physical locations of Fe and Cr(VI) did not coincide for the most part. The reason for this appears to be that Fe was mostly contained within the larger soil grains, while Cr(VI) was preferentially

located within the finer grained regions (see Fig. 5). Thus, Cr(VI) sorption on iron hydroxides is considered to be a secondary (if not minor) binding mechanism in this soil, with interstitial PbCrO₄ precipitation as the main immobilization mechanism. This observation corroborates with the SPLP Cr(VI) leaching data for the untreated unsaturated soil; the Cr(VI) concentration of 0.2 mg/L in the leachate coincides with the solubility of Cr(VI) with respect to PbCrO₄.

4. Conclusions

In this study, it was attempted to treat a Cr-contaminated aquifer soil by simple pH buffering, the rationale being to immobilize the predominant Cr(III) (~500 mg/kg compared to 30 mg/kg Cr(VI)). The addition of lime increased soil pH to >12 as expected, but CO₂ sequestration decreased soil pH to 9 over 1 year. The addition of potassium carbonate increased soil pH to 10 and no substantial acidification mechanism was observed within 1 year of monitoring. The effect of washing-out by groundwater seepage could be an additional buffering mechanism that was not captured in this study. In any case, the treatment approach failed because the complete mobilization of Cr(VI) proved to be prohibitive without additional reductive treatment.

Reductive treatment of the high-Cr(VI) (8000 mg/kg) near-surface soil using calcium polysulfide showed that this soil was extremely difficult to treat and that the addition of the reducing agent initially caused an apparent mobilization of Cr(VI) in the SPLP test. Alkaline digestion and SPLP were both found to be unreliable tests in predicting actual Cr speciation, with ongoing reduction during the tests. Polysulfides were shown to have substantial “staying” power, with the redox potential remaining low up to 180 days for the 2X dosage, even in the presence of oxygen. The extreme low solubility of Cr(VI) in this soil renders the addition of a slow-reacting reductant necessary, if the reduction avenue is to be pursued.

The application of synchrotron micro-X-ray techniques (μ XRF, μ XANES, μ XRD) on the treated near-surface soil at 60 days curing showed that some reduction had taken place compared to the control sample, but also that the bulk of the Cr(VI) remained largely unreacted. Especially high-Cr(VI) areas, shown to be lead chromate, were recalcitrant to treatment. PbCrO₄ precipitated in the interstitial pores of the soil, so that Cr(VI) was predominantly associated with the fine-grained material between larger soil grains; little Cr(VI) was found diffuse within larger particles. Even though this was encouraging in terms of mass transfer considerations, the extremely low solubility of PbCrO₄ ultimately rendered reductive treatment unattractive. Since Pb was found only in the top 5 ft of the site, it is considered that removal and disposal or capping of this portion is a more cost-effective alternative than treatment, while reductive treatment of deeper zones and especially the aquifer soil with calcium polysulfide remains a viable alternative.

Acknowledgements

We wish to thank John Miller and National Chromium Inc., for the financial support of the investigation. Luke Hellerich of AECOM provided valuable input and guidance for the site investigation and treatment design. We thank Rick Wilkin of U.S.EPA for providing the XANES spectrum of Cr(VI) sorbed on goethite. Sirine Fakra and Matthew A. Marcus of LBNL provided continuous support for the μ XAS data acquisition, analysis and interpretation. ALS-LBNL operations are supported by the Director, Office of Science, Office of Basic Energy Sciences, US Department of Energy under contract number DE-AC02-05CH11231.

References

- [1] D. Rai, L.E. Eary, J.M. Zachara, Environmental chemistry of chromium, *Sci. Tot. Environ.* 86 (1989) 15–23.
- [2] L.A. Hellerich, N.P. Nikolaidis, Studies of hexavalent chromium attenuation in redox variable soils obtained from a sandy to sub-wetland groundwater environment, *Water Res.* 39 (2005) 2851–2868.
- [3] L.A. Hellerich, N.P. Nikolaidis, G.M. Dobbs, Evaluation of the potential for natural attenuation of hexavalent chromium within a sub-wetland groundwater, *J. Environ. Manage.* 88 (4) (2008) 1513–1524.
- [4] B. Faybishenko, T.C. Hazen, P.E. Long, E.L. Brodie, M.E. Conrad, S.S. Hubbard, J.N. Christensen, D. Joyner, S.E. Borglin, R. Chakraborty, K.H. Williams, J.E. Peterson, J. Chen, S.T. Brown, T.K. Tokunaga, J. Wan, M. Firestone, D.R. Newcomer, C.T. Resch, K.J. Cantrell, A. Willett, S. Koenigsberg, In situ long-term reductive bioimmobilization of Cr(VI) in groundwater using hydrogen release compound, *Environ. Sci. Technol.* 42 (22) (2008) 8478–8485.
- [5] USEPA, In Situ Treatment of Soil and Groundwater Contaminated with Chromium: Technical Resource Guide EPA 625/R-00/004, October 2000.
- [6] P. Storch, A. Messer, D. Palmer, R. Pyrih, Pilot test for in situ geochemical fixation of chromium (VI) using calcium polysulfide, in: Proceedings of the Third International Conference on Remediation of Chlorinated and Recalcitrant Compounds, Battelle Press, Monterey, CA, 2002.
- [7] FRTR (Federal Remediation Technologies Roundtable), Abstracts of Remediation Case Studies Volume 8, EPA 542-R-04-012, June 2004.
- [8] IETEG (Independent Environmental Technical Evaluation Group), in: J. Guertin, J.A. Jacobs, C. Avakian (Eds.), Chromium(VI) Handbook, CRC Press, Boca Raton, FL, 2005.
- [9] B. Charboneau, K.M. Thomson, R. Wilde, B. Ford, M. Gerber, Hanford groundwater remediation, in: Proceedings of the WM'06 Conference, Tuscon, AZ, February 26–March 2, 2006.
- [10] M.C. Graham, J.G. Farmer, P. Anderson, E. Paterson, S. Hillier, D.G. Lumsdon, R.J.F. Bewley, Calcium polysulfide remediation of hexavalent chromium contamination from chromite ore processing residue, *Sci. Tot. Environ.* 364 (2006) 32–44.
- [11] M. Wazne, S.C. Jagupilla, D.H. Moon, S.C. Jagupilla, C. Christodoulatos, M.G. Kim, Assessment of calcium polysulfide for the remediation of hexavalent chromium in chromite ore processing residue (COPR), *J. Hazard. Mater.* 143 (2007) 620–628.
- [12] D.H. Moon, M. Wazne, S.C. Jagupilla, C. Christodoulatos, M.G. Kim, A. Koutsospyros, Particle size and pH effects on remediation of chromite ore processing residue (COPR) using calcium polysulfide (CaS₅), *Sci. Tot. Environ.* 399 (2008) 2–10.
- [13] N.P. Nikolaidis, G.A. Robbins, M. Scherer, B. McAninch, G. Binkhorst, J. Asikainen, S.L. Suib, Vertical distribution of chromium and partitioning in a glaciofluvial aquifer, *Ground Water Monit. Rem.* 14 (3) (1994) 150.
- [14] N.P. Nikolaidis, L.A. Hellerich, J.A. Lackovic, Methodology for site-specific, mobility-based cleanup standards for heavy metals in glaciated soils, *Environ. Sci. Technol.* 33 (1999) 2910–2916.
- [15] International Centre for Diffraction Data (ICDD), Powder Diffraction File, PDF-2, 2002.
- [16] M.A. Marcus, A.A. MacDowell, R. Celestre, A. Manceau, T. Miller, H.A. Padmore, R.E. Sublett, Beamline 10.3.2 at ALS: a hard X-ray microprobe for environmental and materials sciences, *J. Synchrotron. Radiat.* 11 (2004) 239–247.
- [17] S. Kraft, J. Stümpel, U. Kuetsgens, High resolution X-ray absorption spectroscopy with absolute energy calibration for the determination of absorption edge energies, *Rev. Sci. Instrum.* 67 (3) (1996) 681–687.
- [18] A.P. Hammersley, FIT2D V9.129 – Reference Manual V3.1, vol. 346 ESRF Internal Report – ESRF98HA01T, 1988.
- [19] P.R. Bloom, U.L. Skyllberg, M.E. Sumner, Soil acidity, in: Chemical Processes in Soils, SSSA Book Series No. 8, 2005, p. 411.
- [20] V.L. Snoeyink, D. Jenkins, *Water Chemistry*, John Wiley and Sons, New York, 1980.
- [21] M.R. Hausmann, *Engineering Principles of Ground Modification*, McGraw Hill, New York, 1990.
- [22] O.K. Borggaard, Effect of surface area and mineralogy of iron oxides on their surface charge and anion-adsorption properties, *Clays Clay Min.* 31 (1983) 230–232.
- [23] D.W. King, Role of carbonate speciation on the oxidation rate of Fe(II) in aquatic systems, *Environ. Sci. Technol.* 32 (1998) 2997–3003.
- [24] D. Dermatas, M. Chrysochoou, D.H. Moon, D.G. Grubb, M. Wazne, C. Christodoulatos, Ettringite-induced heave in chromite ore processing residue (COPR) upon ferrous sulfate treatment, *Environ. Sci. Technol.* 40 (18) (2006) 5786–5792.
- [25] D. Dermatas, G. Shen, M. Chrysochoou, D.G. Grubb, N. Menounou, P. Dutko, Pb speciation vs. TCLP release in army firing range soils, *J. Hazard. Mater.* 136 (1) (2006) 34–46.
- [26] D. Dermatas, M. Chrysochoou, D.G. Grubb, X. Xu, Phosphate treatment of range soils: Pb fixation or P release? *J. Environ. Qual.* 37 (2008) 47–56.
- [27] M. Chrysochoou, S. Fakra, M.A. Marcus, D.H. Moon, D. Dermatas, Microstructural analyses of Cr(VI) speciation in chromite ore processing residue (COPR), *Environ. Sci. Technol.* 43 (14) (2009) 5461–5466.